Journal of Solid State Chemistry **144,** 125–135 (1999)
Article ID jssc.1999.8132, available online at http://www.idealibrary.com on IDEAL®

$Sr_4Ru_{3.05}O_{12}$: A New Member of the Hexagonal Perovskite Family

C. Renard, S. Daviero-Minaud, M. Huvé, and F. Abraham[1]

Laboratoire de Cristallochimie et Physicochimie du Solide, URA CNRS 452, ENSCL, Université des Sciences et Technologies de Lille, BP 108, 59652 Villeneuve d'Ascq Cedex, France

Received April 21, 1998; in revised form December 31, 1998; accepted January 5, 1999

$Sr_4Ru_{3.05}O_{12}$ crystals have been synthesized under hydrothermal conditions (500°C, 1800 bars). The crystal structure was determined by X-ray single-crystal diffraction. The unit cell is hexagonal and presents a superstructure ($a_s = \sqrt{3}a_b =$ 9.641(2) Å and $c_s = c_b =$ 18.186(5) Å. The average structure has been determined ($P6_3mc$ space group, $a_b =$ 5.566(4) Å, $c_b =$ 18.186(5) Å, and $Z = 2$). The structure refinement converged to $R = 0.057$ and $R_w = 0.032$ for 186 independent reflections. The crystal structure is based on the 8H $(cchc)_2$ close-packed stacking of SrO_3 layers with face-sharing octahedra partially occupied by the ruthenium atoms. Electron diffraction observations and high-resolution electron microscopy image observations recognize the X-ray average structure. The superstructure spots appear clearly in the ED patterns and most of the crystals display diffuse streaks along c^*, which are consistent with the disorder clearly imaged in the HREM images. Heating $Sr_4Ru_{3.05}O_{12}$ crystals leads to the disappearance of the superstructure. © 1999 Academic Press

INTRODUCTION

A large number of oxide compounds whose structures were derived from the cubic or hexagonal perovskite structure AMO_3 have been reported and widely studied. Their structures are built on the close-packed stacking of AO_3 layers (1). Between two layers, the oxygen atoms form octahedral sites occupied by the M cations. Numerous different stacking sequences of A, B, or C layers are possible. They give rise to various frameworks, where the octahedra can be isolated or they can share either corner (cubic close packing) or face (hexagonal close packing). The crystal structures of the Ba–Ru–O compounds system are some examples. The study of the Sr–Ru–O system has permitted one to isolate various compounds. $SrRuO_3$ (2) and $Sr_4Ru_2O_9$ (3) crystallize with a pseudo-cubic perovskite and hexagonal perovskite structures, respectively. The other ruthenium oxides, the $Sr_{n+1}Ru_nO_{3n+1}$ family ($n = 1$ (4), 2 (4)), derive from the K_2NiF_4 structure but they can be described by the stacking of $Sr_{n+1}O_{3n+1}$ layers. All these oxides contain tetravalent or pentavalent ruthenium in octahedral coordination. $SrRuO_4 . H_2O$, a ruthenium VI hydrated oxide, has also been reported in the literature (5) but without any information on its crystal structure. In fact, by comparison with the barium analogous compound (6), the actual formula would be $SrRuO_3(OH)_2$ to emphasize the presence of the trigonal bipyramidal $[RuO_3(OH)_2]^{2-}$ ion.

All the Sr–Ru–O compounds known up to today have been synthesized under atmospheric pressure. In order to obtain new strontium ruthenium oxides with higher valency ruthenium, hydrothermal syntheses were employed. Hydrothermal conditions in the 1 to 10 kbars pressure range is a good way to prepare high valency oxide (7). This paper reports the preparation and crystal structure of a new crystalline phase with the $Sr_4Ru_{3.05}O_{12}$ formula.

EXPERIMENTAL

Synthesis

The $Sr_4Ru_{3.05}O_{12}$ crystals were synthesized under hydrothermal conditions. High-temperature, high-pressure synthesis was performed in a sealed gold tube in a Novaswiss autoclave. The compound was obtained by heating a mixture of 0.133 g of $Sr(OH)_2 . 8H_2O$, 0.033 g of RuO_2, 0.030 g of $KClO_3$, and 0.5 mL of distilled water to 500°C, under 1800 bars, during 72 h. The heating of the furnace was then turned off. The product was washed with a 0.1 M HCl solution, to eliminate the excess of strontium carbonate, and was then filtered and dried. Black hexagonal platelet crystals were found. Small single crystals of $Sr_4Ru_{3.05}O_{12}$ can also be obtained from SrO_2, RuO_2, and distilled water or from $Sr(OH)_2 . 8H_2O$, RuO_2, and water without $KClO_3$. But the first-described synthesis using $KClO_3$ is the only one which gave large enough single crystals suitable for a structural determination from X-ray single-crystal diffraction data.

[1]To whom correspondence should be addressed. E-mail: abraham@ensc-lille.fr.

0022-4596/99 $30.00

Single-Crystal X-Ray Diffraction

A small hexagonal platelet crystal of 34 μm thick and 80 μm for the greatest dimensions was selected for X-ray intensities measurements. Oscillation and Weissenberg photographs have shown a 6/*mmm* Laue symmetry and unit-cell parameters close to $a_b \approx 5.6$ Å and $c_b \approx 18.2$ Å. They display the existence of a superstructure with $a_s = a_b\sqrt{3} \approx 9.6$ Å. The superstructure unit vectors are related to the substructure unit vectors by

$$\begin{pmatrix}\mathbf{a}_s\\ \mathbf{b}_s\\ \mathbf{c}_s\end{pmatrix} = \begin{pmatrix}2 & 1 & 0\\ \bar{1} & 1 & 0\\ 0 & 0 & 1\end{pmatrix}\begin{pmatrix}\mathbf{a}_b\\ \mathbf{b}_b\\ \mathbf{c}_b\end{pmatrix}.$$

Intensity data for $Sr_4Ru_{3.05}O_{12}$ were collected at room temperature using a CAD-4 Enraf Nonius diffractometer with graphite monochromated Mo$K\alpha$ radiation. Accurate lattice parameters were obtained from a least-squares refinement with 25 automatically centered reflections, $a =$ 9.641(2) Å and $c = 18.186(5)$ Å. The intensities data were collected for one half of the reciprocal lattice in the range $2^\circ < \theta < 25^\circ$ for the superstructure cell. A total of 6726 reflections were recorded, which were further corrected for Lorentz and polarization effects. Absorption corrections were applied using the analytical method of De Meulenaer and Tompa (8) with $\mu = 265\ \text{cm}^{-1}$ and the data were averaged in the 6/*mmm* Laue symmetry ($R_{\text{int}} = 0.036$). Details of data collection and refinement are given in Table 1. The structure was solved and refined in the basic lattice. Examination of the collected data indicated that the conditions for the observed reflections are $000l$, $l = 2n$ and $hh2\bar{h}l$, $l = 2n$. Thus, the possible space groups are $P6_32c$, $P6_3mc$, and $P6_3/mmc$.

Transmission Electron Microscopy

The transmission electron microscopy study has been performed with a Jeol 200CX. High-resolution images were

TABLE 1
Crystallographic Parameters for $Sr_4Ru_{3.1}O_{12}$

	Superstructure	Basic structure
	Crystal data	
Crystal system	hexagonal	hexagonal
Laue group	6/*mmm*	6/*mmm*
Space group	$P6_3cm$	$P6_3mc$
Cell dimensions	$a = 9.641(2)$ Å, $c = 18.186(5)$ Å	$a = 5.566(2)$ Å, $c = 18.186(5)$ Å
Volume (Å^3)	1463.9	488.0
Z	6	2
Density	5.81	5.81
	Data collection	
Equipment	Nonius CAD4	
λ (Mo$K\alpha$), Å	0.7107	
Scan technique	ω–2θ	
θ range	2°–25°	
Recording reciprocal space	$-12 \le h \le 12$ $-12 \le k \le 12$ $0 \le 1 \le 23$	
Number of measured reflections	6726	1535
Number of observed reflections $I > 3\sigma(I)$	2128	1196
Number of unique data	364	186
μ (cm^{-1}) (for λ Mo$K\alpha = 0.7107$)	265	265
Limiting faces and distances (cm) from an arbitrary origin	001, 00$\bar{1}$: 0.0017	001, 00$\bar{1}$: 0.0017
	$2\bar{1}\pm3$, 11 ± 3, $\bar{1}2\pm3$, $\bar{2}1\pm3$, $\bar{1}\bar{1}\pm3$, $1\bar{2}\pm3$: 0.0031	10 ± 3, 01 ± 3, $\bar{1}1\pm3$, $\bar{1}0\pm3$, $0\bar{1}\pm3$, $1\bar{1}\pm3$: 0.0031
Transmission factors	0.232–0.444	0.232–0.444
Merging R factor	0.036	0.030
	Structure solution and refinement	
Number of refined parameters		28
R		0.057
R_w ($w = 1/\sigma(F_0)$)		0.032

obtained using a Jeol 4000EX instrument, from finely crushed hexagonal platelet crystals dispersed on copper grids.

Powder X-Ray Diffraction

Powder X-ray diffraction profiles were recorded on a Siemens D5000 diffractometer (Cu$K\alpha$ radiation) equipped with a back monochromator.

Thermal Analysis

The DSC analyses were performed on a 141 SETARAM analyzer and the thermogravimetric analyses on a simultaneous TG-DTA 92-1600 SETARAM thermobalance.

Magnetic Measurements

The magnetic susceptibility of the samples was measured using a superconducting quantum interference device SQUID magnetometer. Measurements were taken under 0.2 T in the temperature range $5 < T < 300$ K, that is to say a field cooling cycle. No correction was made for the applied field diamagnetic contribution of the different cations.

RESULTS AND DISCUSSION

Structure Determination

The structure was solved by the heavy atom method. The hexagonal lattice with parameters $a_b = 5.566(2)$ Å and $c = 18.186(5)$ Å allows one to connect this compound to the hexagonal perovskite-like structures with an eight-layers sequence. The Patterson map confirms an eight-layers sequence, and the possible space groups lead to a $(cchc)_2$ sequence of close-packed stacking of SrO_3 layers. Strontium and ruthenium positions corresponding to this crystal structure model were refined in each space group. The best refinement was obtained in the $P6_3mc$ space group. At this stage of the study, the high value of Ru(3) and Ru(4) thermal vibration parameters leads to partial occupancy of the corresponding sites by ruthenium atoms. The oxygen atom's positions were subsequently located from Fourier difference maps. The ruthenium occupancy factors were then refined to 0.50(3) and 0.55(3) for Ru(3) are Ru(4), respectively. These values yielded to $R = 0.057$ and $R_w = 0.032$. The structure refinement leads to the $Sr_4Ru_{3.05}O_{12}$ formula. We note that Sr(2) and oxygen atoms have high thermal parameters. These values can be explained by the strains imposed by the basic structure. The final positional parameters and isotropic temperature factors for $Sr_4Ru_{3.05}O_{12}$ basic structure are listed in Table 2. For the superstructure refinement in the $P6_3cm$ space group compatible with the extinction conditions observed, the atomic positions were deduced from the basic structure results. The refinement of these data did not give satisfying results. The refinement does not converge and the thermal parameters of the ruthenium atoms are very low, on the other hand, the thermal factors of the oxygen atoms are very high. Only the strontium atom positions are properly refined. Unfortunately the superstructure refinement failed and did not allow an explanation of the observed superstructure. However, the results seem to indicate that the strontium atoms do not impose the superstructure.

TABLE 2
Atomic and Thermal Parameters for $Sr_4Ru_{3.05}O_{12}$

Atom	Position type	Occupancy factor	x	y	z	B
Sr(1)	2*a*	1	0	0	0	1.3(1)
Sr(2)	2*b*	1	2/3	1/3	0.125(1)	3.4(3)
Sr(3)	2*b*	1	1/3	2/3	0.239(1)	1.2(1)
Sr(4)	2*b*	1	2/3	1/3	0.3560(8)	1.3(3)
Ru(1)	2*b*	1	1/3	2/3	0.0533(7)	0.2(1)
Ru(2)	2*b*	1	1/3	2/3	0.4292(7)	0.4(1)
Ru(3)	2*a*	0.50(3)	0	0	0.1756(8)	0.9(4)
Ru(4)	2*a*	0.55(3)	0	0	0.3094(8)	0.1(3)
O(1)	6*c*	1	0.518(7)	− 0.518	− 0.002(2)	3.1(5)
O(2)	6*c*	1	0.176(4)	− 0.176	0.122(2)	3.7(9)
O(3)	6*c*	1	0.839(2)	− 0.839	0.249(2)	2.1(4)
O(4)	6*c*	1	0.166(4)	− 0.166	0.380(2)	2.6(7)

$Sr_4Ru_{3.05}O_{12}$ structure is a $(cchc)_2$ 8H hexagonal polytype perovskite structure; it is built on the stacking of SrO_3 layers with an *ABCBACBC* sequence. Figure 1 presents the

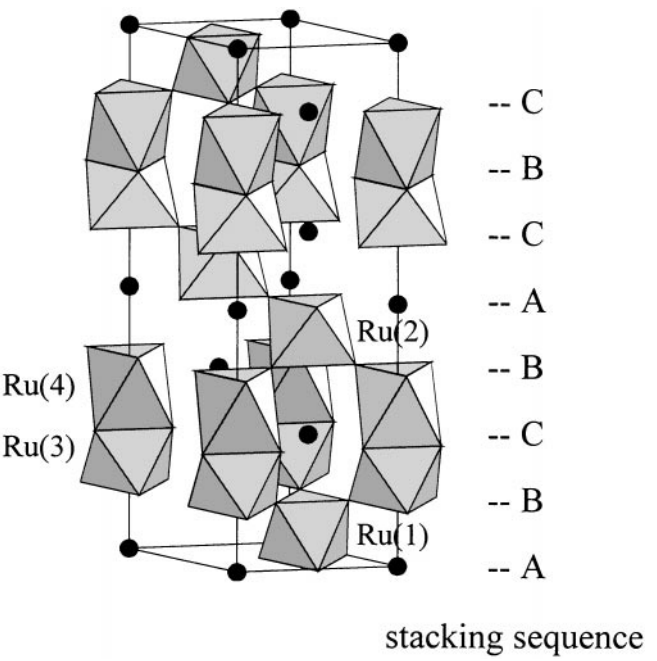

FIG. 1. Perspective view of the $Sr_4Ru_{3.05}O_{12}$ basic structure.

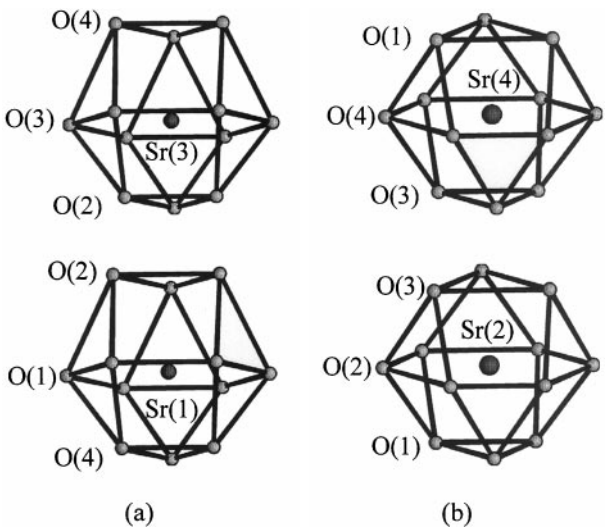

FIG. 2. Coordination polyhedron of strontium atoms in $Sr_4Ru_{3.05}O_{12}$. (a) Sr(1) and Sr(3) environments correspond to a hexagonal close packed structure. (b) Sr(2) and Sr(4) environments correspond to cubic close packed structure.

TABLE 3
Main Interatomic Distances in $Sr_4Ru_{3.05}O_{12}$

Bond	Distance, Å	Bond	Distance, Å
Sr(1)–O(1)(6 ×)	2.80(3)	Sr(2)–O(1)(3 ×)	2.72(5)
–O(2)(3 ×)	2.79(3)	–O(2)(6 ×)	2.78(2)
–O(4)(3 ×)	2.71(3)	–O(4)(3 ×)	2.80(3)
Sr(3)–O(2)(3 ×)	2.61(4)	Sr(4)–O(1)(3 ×)	3.14(5)
–O(3)(6 ×)	2.79(1)	–O(3)(3 ×)	2.56(3)
–O(4)(3 ×)	3.031(4)	–O(4)(6 ×)	2.82(3)
Ru(1)–O(1)(3 ×)	2.04(5)	Ru(2)–O(1)(3 ×)	1.90(5)
–O(2)(3 ×)	1.96(3)	–O(4)(3 ×)	1.84(3)
Ru(3)–O(2)(3 ×)	1.95(3)	Ru(4)–O(3)(3 ×)	1.95(2)
–O(3)(3 ×)	2.05(3)	–O(4)(3 ×)	2.08(3)
Ru(3)–Ru(4)	2.40(2)		

basic structure framework. The strontium atoms are 12-coordinated with the two classical coordination polyhedra corresponding to cubic and hexagonal close-packed structures (Fig. 2). The ruthenium atoms occupy the octahedral site created by the oxygen atoms between the layers. Two octahedra on both sides of an *h* layer are face-shared when octahedra on both sides of a *c* layer are corner-shared. Thus, the *cchc* stacking sequence generates pairs of face-sharing octahedra which form dimeric units partially occupied by Ru(3) and Ru(4) atoms. Corner-sharing octahedra, Ru(1)O6 and Ru(2)O6, connect these units. The main interatomic distances are reported in Table 3. The main oxidation state of the ruthenium is 5.25; however, the accuracy of the Ru–O distances for the mean structure does not allow one to hypothesize on the individual oxidation degrees of each ruthenium atom.

The Ru_2O_9 dimers are typical of many barium ruthenium compounds such as $Ba_3Ru_2MO_9$ (M = Ni, Co, Zn (9), In (10), Mg, Ca (11), Sr (12)), $Ba_4Ru_3MO_{12}$ (M = Li, Na, Mg, Zn) (13), $Ba_5Ru_2O_{10}$ (14), or 4H $BaRuO_3$ (15). The Ru–Ru distance in these dimers depends on the ruthenium oxidation state: 2.47 to 2.5 Å for Ru^{4+} and 2.66 to 2.78 Å for Ru^{5+} (15). The short metal–metal distance in tetravalent ruthenium compounds indicates a Ru–Ru bonding, whereas the electrostatic repulsion between two pentavalent ruthenium atoms prevents the bond formation. We observe that, in all cases, the metal–metal distance is longer than the distance between two BaO_3 layers (around 2.3 Å). In the pairs of face-sharing octahedra, the ruthenium atoms are not in the center of the polyhedra but are shifted toward the unshared oxygen atoms. This shift increases the Ru–Ru distance, which becomes longer than the interlayer distance. The very short distance between two SrO_3 layers (around 2 Å) does not favor the formation of dimeric units, which would contain important metal–metal repulsion or would lead to an important distortion of the octahedra.

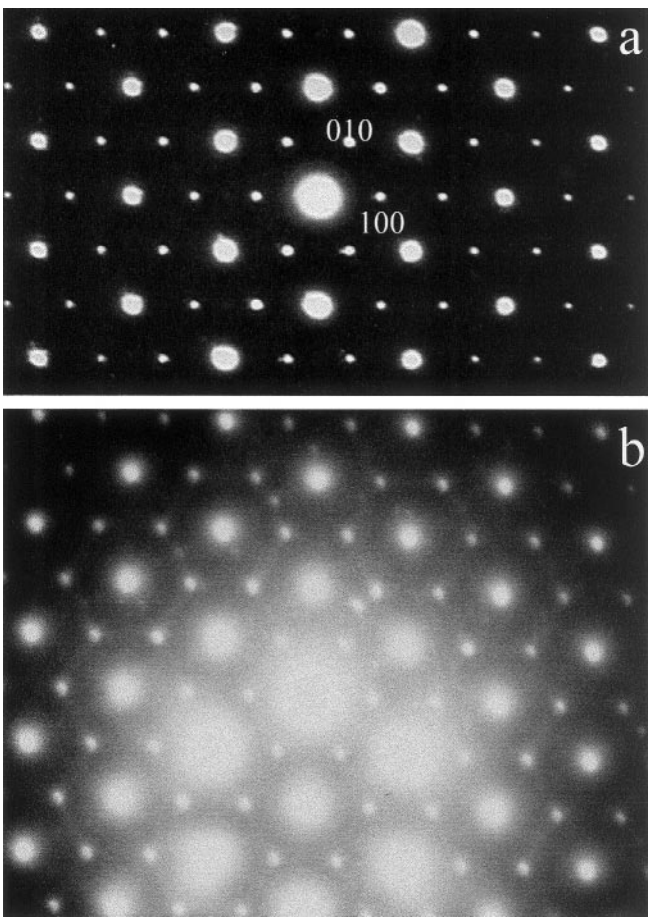

FIG. 3. [0001] EDP for $Sr_4Ru_{3.05}O_{12}$, (a) perfect pattern, (b) pattern with diffuse streaks.

In the Sr–Ru–O system, $Sr_4Ru_2O_9$ is currently the only reported compound containing pairs of face-sharing octahedra. The ruthenium is pentavalent and the metal–metal distances are 2.768(6) and 2.781(3) Å for the two independent Ru(1) and Ru(2) atoms. These values, higher than the interlayer distance (2.026 Å), show that the ruthenium atoms are shifted from the center of the octahedra. In $Sr_4Ru_{3.05}O_{12}$, the ruthenium atoms are near the center of the octahedra and the Ru(3)–Ru(4) distance (2.40 Å) is very close to the distance between the center of the two face-sharing octahedra (2.35 Å). This means that only one dimeric unit octahedron is occupied by the ruthenium. It is in good agreement with the refined occupation rate: 50(3)% for Ru (3) and 55(3)% for Ru (4). The majority of the dimeric units are half filled: $Ru\square O_9$, $\square$ represents a vacancy. For the little proportion of the fully occupied face-sharing octahedra Ru_2O_9, we can suppose that the ruthenium atoms are shifted from the center of the octahedron to increase the metal–metal distance. But the basic structure refinement gives an average position for the ruthenium atoms and does not allow one to distinguish the two sorts of dimers.

Electron Microscopy

In order to explain the difficulties encountered for the superstructure refinement, a TEM study has been performed. The electron diffraction patterns (EDP) confirm the superstructure unit-cell dimensions, the observed extinction conditions on these patterns are in accordance with the $P6_3cm$ space group. The superstructure spots are particularly evidenced on the [0001] EDP (Fig. 3a). All the EDP are indexed in the superstructure cell. The first hexagon

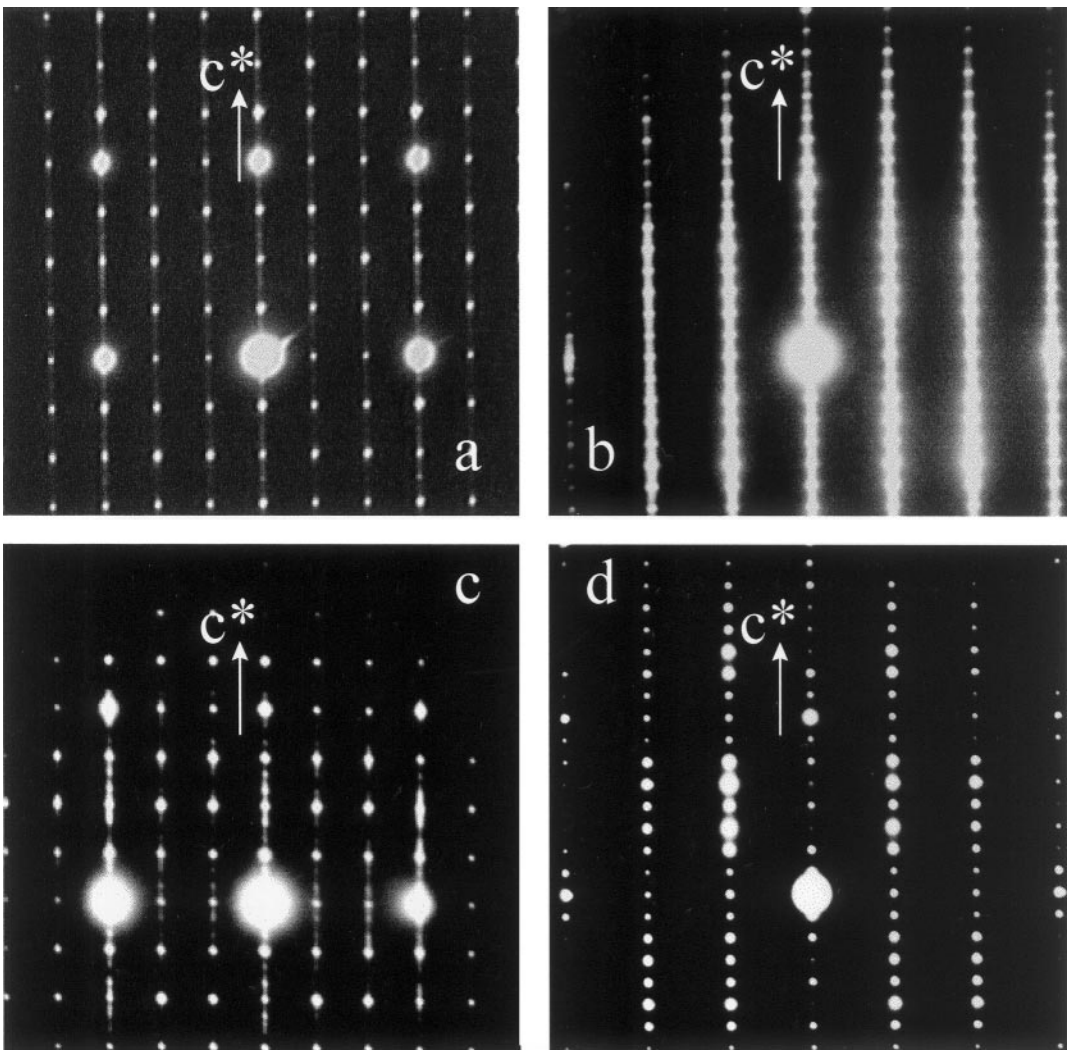

FIG. 4. The [100] and [110] EDP for $Sr_4Ru_{3.05}O_{12}$ presented in (a) and (b), respectively, exhibit diffuse streaks. The [110] EDP can often display supplementary spots (c).

spots are less intense than the second spots and correspond to the superstructure spots. Although the majority of the [0001] EDP are perfect, few of them display weak diffuse streaks revealing some disorder in this plane (Fig. 3b). The [0001] HREM image corresponding to the EDP of Fig. 3a is defect free. However, streaks can often be observed along c^*. In most cases, the $[10\bar{1}0]$ and $[11\bar{2}0]$ EDP exhibit diffuse streaks more or less intense (Figs. 4a–c). Sometimes supplementary spots are observed (Fig. 4c) or no defect appears (Fig. 4d). From the electron diffraction study, it is obvious that the preparation is not homogeneous.

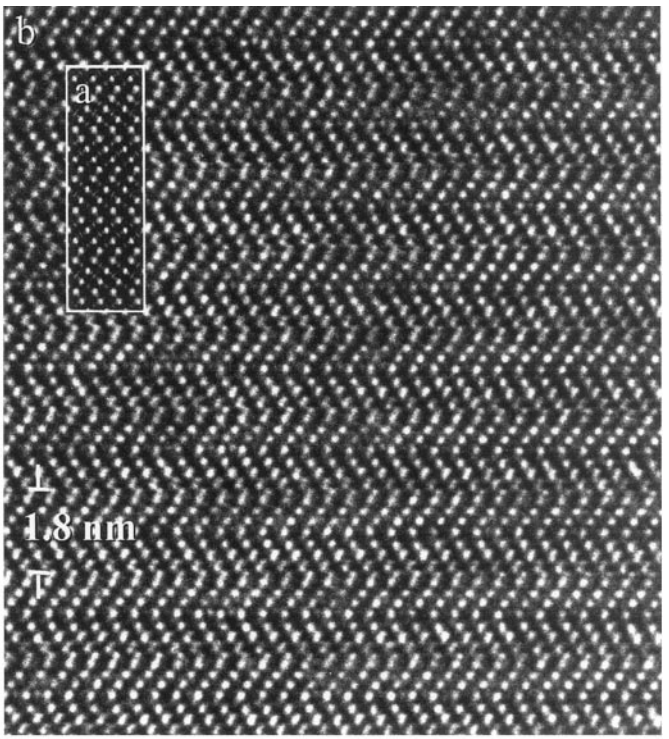

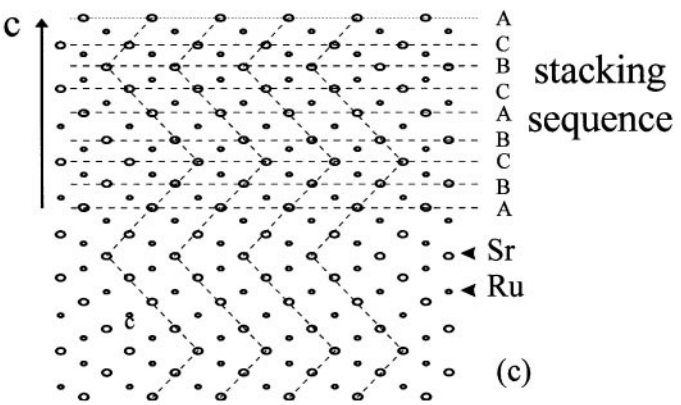

FIG. 5. Experimental and simulated [100] HREM images for $Sr_4Ru_{3.05}O_{12}$. Comparison between the projection of the structure and the corresponding [100] HREM image.

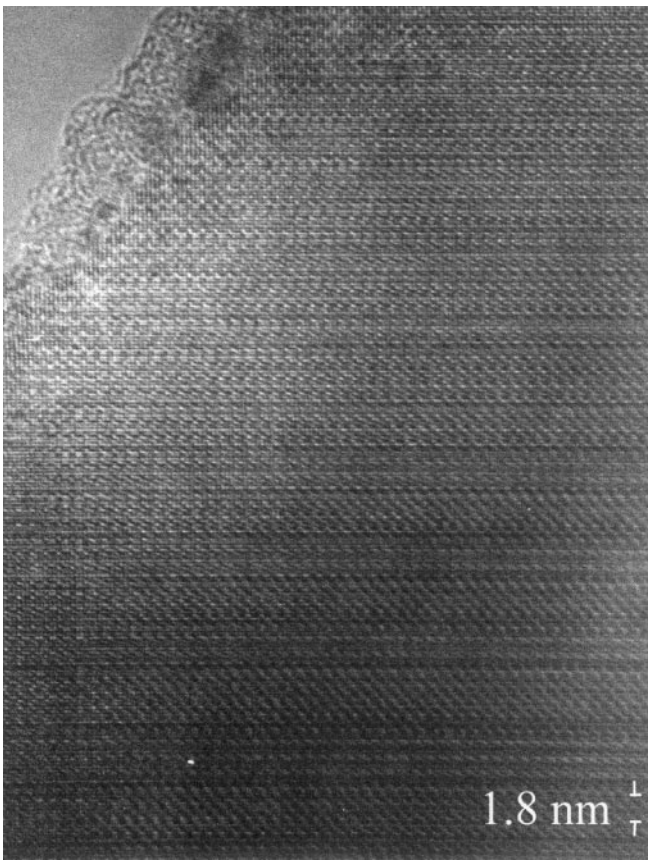

FIG. 6. Typical experimental [110] HREM image for $Sr_4Ru_{3.05}O_{12}$.

The $[10\bar{1}0]$ HREM image corresponding to the non-defect EDP displays regular zigzag or chevron along c. This typical contrast has already been observed for isotype compounds (16,17). Computer-simulated images were calculated on the basis of the refined position parameters of the basic structure. For a defocus of -650 Å and a thickness of 80 Å, the agreement between the calculated and experimental images is striking. For these conditions of defocus and thickness the strontium ions are highlighted as bright dots and the correlation with the projection of the structure is direct (Fig. 5). But for most of the crystals, the c^* is not perfect and the $[11\bar{2}0]$ image corresponding to the EDP of Fig. 4c illustrates this phenomenon; the image evidenced irregularities along the c axis (Fig. 6). According to the HREM images, the stacking sequence of SrO_3 layers is not modified in the superstructure. The structure is always a $(cchc)_2$ 8H hexagonal perovskite structure, but for most of the crystals the c^* direction exhibits diffuse streaks which can be associated with a disorder in the cations occupation of the face-sharing octahedra. It explains the difficulties encountered for the superstructure refinement from X-ray single-crystal data. The HREM images have shown that the

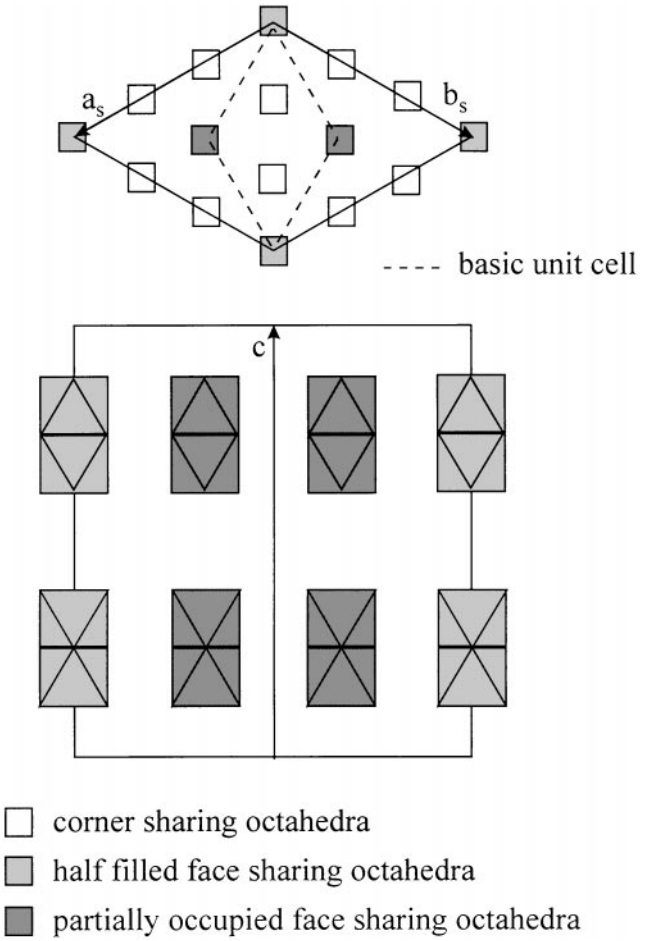

FIG. 7. Schematic representation of the $Ba_8Ta_6NiO_{24}$ and $Ba_8Ta_4Ti_3O_{24}$ crystal superstructure.

stacking sequence of SrO_3 layers is still $(cchc)_2$; thus, the ruthenium atoms impose the superstructure.

$Sr_4Ru_{3.05}O_{12}$ is isostructural with $Ba_8Ta_6NiO_{24}$ (16) and $Ba_8Ta_4Ti_3O_{24}$ (17) and is closely related to $Ba_{10}Ta_{7.04}Ti_{1.2}O_{30}$ (17). These compounds contain partially occupied face-sharing octahedra, which give rise to a superstructure for the two former oxides. The superstructure is imposed by two kinds of dimeric units, one sort centered on 00z and the other centered on 1/3 2/3 z and 2/3 1/3 z of the superstructure cell (Fig. 7). The pairs of face-sharing octahedra are half filled or partially occupied by two cations. Some crystals present stacking sequence defects, in contrast to $Sr_4Ru_{3.05}O_{12}$ crystals that do not present stacking sequence modifications. The presence of partially occupied dimers seems to lead to the formation of defects. On the other hand, the introduction of a second cation with a lower charge, for example in $Ba_4Ru_3MO_{12}$ (M = Li, Na, Mg, or Zn) (11), stabilizes the structure.

Thermal Stability

The D.S.C. analysis of $Sr_4Ru_{3.05}O_{12}$ under air displays a peak at 320°C. The evolution of the powder X-ray diffraction pattern as a function of temperature shows an irreversible transition at about 500°C (Fig. 8). Above this temperature, the superstructure reflections disappear. A thermogravimetric analysis under air indicates that this transition is carried out without weight loss. The heated sample will be called β-$Sr_4Ru_{3.05}O_{12}$. The disappearance of the superstructure reflections is clearer if we compare the room temperature X-ray diffraction patterns of $Sr_4Ru_{3.05}O_{12}$ and β-$Sr_4Ru_{3.05}O_{12}$ and (Fig. 9a). The unit-cell parameters of β-$Sr_4Ru_{3.05}O_{12}$, $a = 5.579(1)$ Å and $c = 18.069(3)$ Å, were obtained from least-squares refinement of X-ray powder data on 26 indexed reflections (Table 4). The c parameter is slightly smaller than the $Sr_4Ru_{3.05}O_{12}$ parameter (18.186 Å). A transmission electron microscopy study of the β phase confirms the X-ray powder results. The [0001] EDP displays the superstructure dots (Fig. 10a), and diffuse streaks appear between the spots. Such streaks also appear along the c^* axis on the $[10\bar{1}0]$ and $[11\bar{2}0]$ EDP (Figs. 10b and 10c) and could be taken to mean a statistical distribution of the ruthenium atoms in the

TABLE 4
Indexing of the X-Ray Powder Diffraction Data for β-$Sr_4Ru_{3.05}O_{12}$

h	k	l	Relative intensity	d_{obs}	d_{calc}
1	0	1	3	4.6674	4.6680
0	0	4	5	4.5119	4.5174
1	0	2	5	4.2633	4.2609
1	0	3	2	3.7678	3.7690
1	0	4	9	3.3014	3.2999
1	0	5	93	2.8944	2.8940
1	1	0	52	2.7902	2.7898
1	0	6	26	2.5569	2.5558
0	0	8	100	2.2584	2.2587
2	0	4	6	2.1308	2.1304
2	0	5	31	2.0087	2.0085
2	0	6	13	1.8845	1.8845
1	0	9	3	1.8544	1.8540
0	0	10	22	1.8067	1.8070
2	1	4	14	1.6925	1.6932
2	1	5	10	1.6300	1.6300
3	0	0	16	1.6109	1.6107
2	1	6	6	1.5620	1.5616
3	0	3	4	1.5556	1.5560
2	0	9	2	1.5439	1.5441
1	1	10	1	1.5158	1.5166
2	0	10	5	1.4472	1.4470
1	0	12	2	1.4380	1.4376
2	2	0	4	1.3950	1.3949

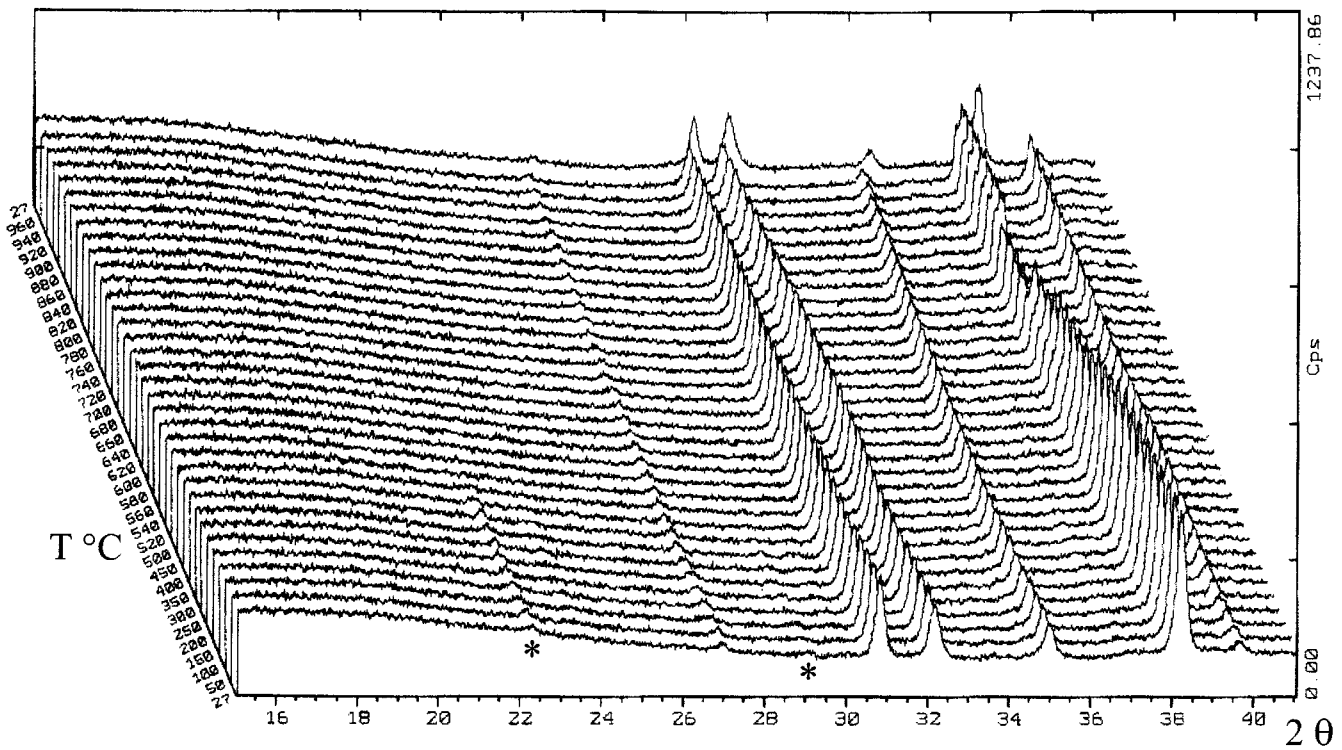

FIG. 8. Powder X-ray diffraction data for $Sr_4Ru_{3.05}O_{12}$ over the temperature range $20 < T < 960°C$. Stars indicate the superstructure reflections.

face-sharing octahedra. After heating, the face-sharing octahedra would be statically occupied by the ruthenium atoms. Thus, the superstructure no longer exists. If we compare the $Sr_4Ru_{3.05}O_{12}$ and β-$Sr_4Ru_{3.05}O_{12}$ X-ray patterns, the heated sample reflections are better defined and thinner than the $Sr_4Ru_{3.05}O_{12}$ patterns. The X-ray pattern

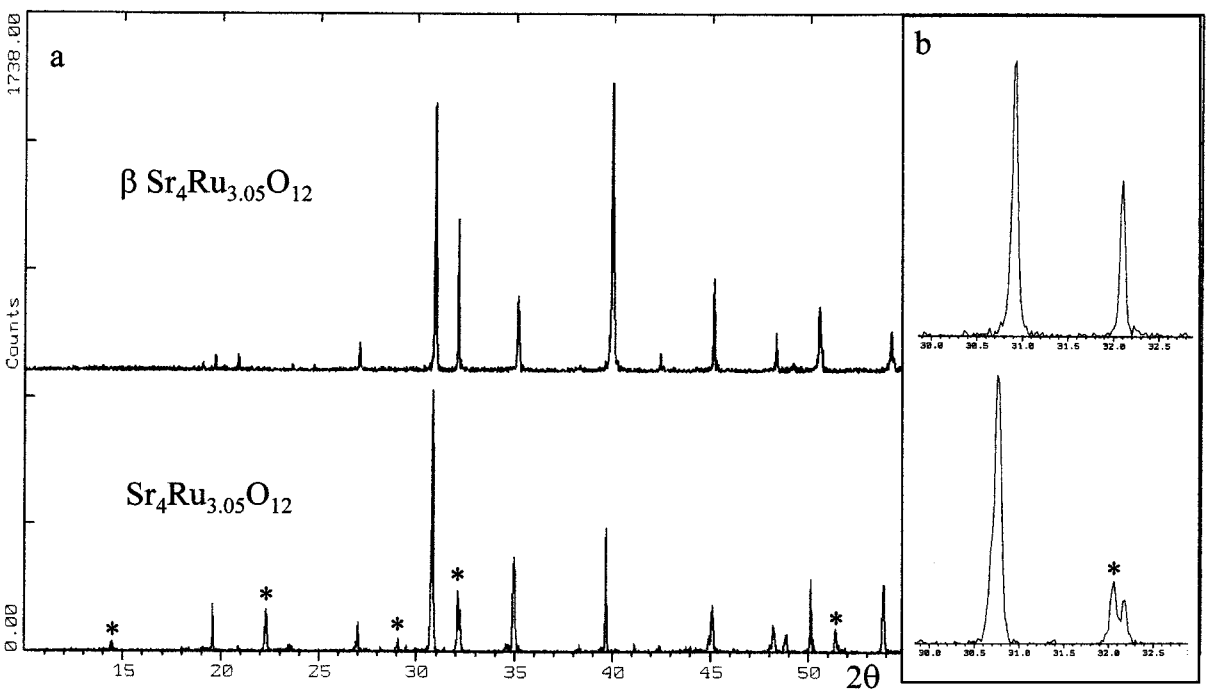

FIG. 9. (a) Powder X-ray diffraction data at room temperature for $Sr_4Ru_{3.05}O_{12}$ and β-$Sr_4Ru_{3.05}O_{12}$, (b) details of the X-ray diffraction profiles.

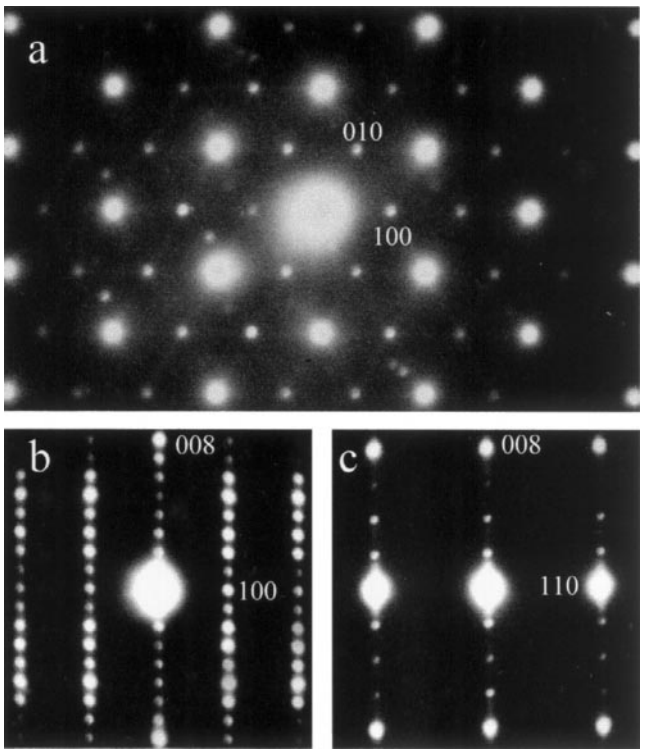

FIG. 10. β-$Sr_4Ru_{3.05}O_{12}$ electron diffraction patterns. (a) [0001] EDP, (b) [100] EDP, (c) [110] EDP.

of $Sr_4Ru_{3.05}O_{12}$ confirms the TEM study, the width of the peaks indicates that the preparation is not homogeneous (Fig. 9b). On the contrary, the X-ray diffraction profile of the heated sample displays thin reflections and indicates that the preparation is homogeneous.

The thermogravimetric analysis under H_2 flow confirms the oxygen content of $Sr_4Ru_{3.05}O_{12}$. The observed weight loss is 15.1% instead of the 15.0% theoretical loss for the $Sr_4Ru_{3.05}O_{12}$ formula. The reduction process leads to a mixture of metallic ruthenium and strontium oxide. The thermogravimetric analysis displays a landing between 270 and 330°C (Fig. 11), corresponding to a weight loss of 8.0%. The X-ray diffraction patterns under a (10%H_2, 90%N_2) flow show clearly the extinction of the $Sr_4Ru_{3.05}O_{12}$ reflections at 170°C and the emergence of reflections of an unidentified new phase from 190 to 280°C, the metallic ruthenium reflections jointly appear weak. After 280°C, the phase is reduced in metallic ruthenium and strontium oxide (Fig. 12). Until now, the intermediate phase has not been isolated at room temperature and under air.

Magnetic Measurements

In order to complete our study, a first magnetic measurement was performed on both compounds: $Sr_4Ru_{3.05}O_{12}$ and the β phase. The thermal variations of the magnetic susceptibility are shown in Figs. 13 and 14, respectively. The variation of the magnetization with H at $T = 10$ K is represented in the inset. The paramagnetic regime is poorly established up to 300 K avoiding the calculation of the mean ruthenium valence. $Sr_4Ru_{3.05}O_{12}$ and the β-phase show a weakly ferromagnetic transition at 185 and 160 K, respectively, which may be due to a ferromagnetic "impurity" or may be intrinsic to our compounds. Effectively, the linear variation of the magnetization showing no saturation until H = 10 T suggests an antiferromagnetic comportment with a small remanent magnetization for the β-phase. This suggests that the magnetic transitions observed are intrinsic to our compound, from a paramagnet to a canted antiferromagnet, as it has already be seen in other Ru^V compounds (18). These results must be confirmed with neutron diffraction studies, which can show magnetic orders and allow us to conclude on the magnetic behavior of our phases.

CONCLUSION

Hydrothermal conditions allow us to synthesize a new strontium ruthenium oxide with a structure based on an 8H close-packing of SrO_3 layers. For the most part, of the pairs of face-sharing octahedra, one octahedron is occupied, whereas the other octahedron is empty. Superstructure reflections indicate that the two different pairs of face-sharing octahedra Ru(3)$\square O_9$ and $\square$Ru(4)O_9 are partially ordered. Statistical disorder of the two pairs occurs at about 320°C and is accompained by the disappearance of the superstructure reflections. This order–disorder distribution was completely confirmed by electron diffraction microscopy. Under reducing atmosphere a new mixed oxide is obtained, and thus is under further investigations. In order to complete the preliminary magnetic study, magnetic measurements at higher temperatures, neutron diffraction, and the thermal variation of the electrical resistivity studies on $Sr_4Ru_{3.05}O_{12}$ and β-phase are needed.

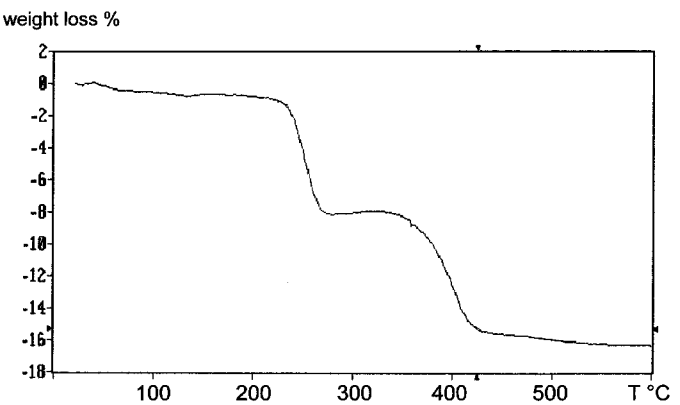

FIG. 11. Thermogravimetric analysis for $Sr_4Ru_{3.05}O_{12}$ under H_2 flow.

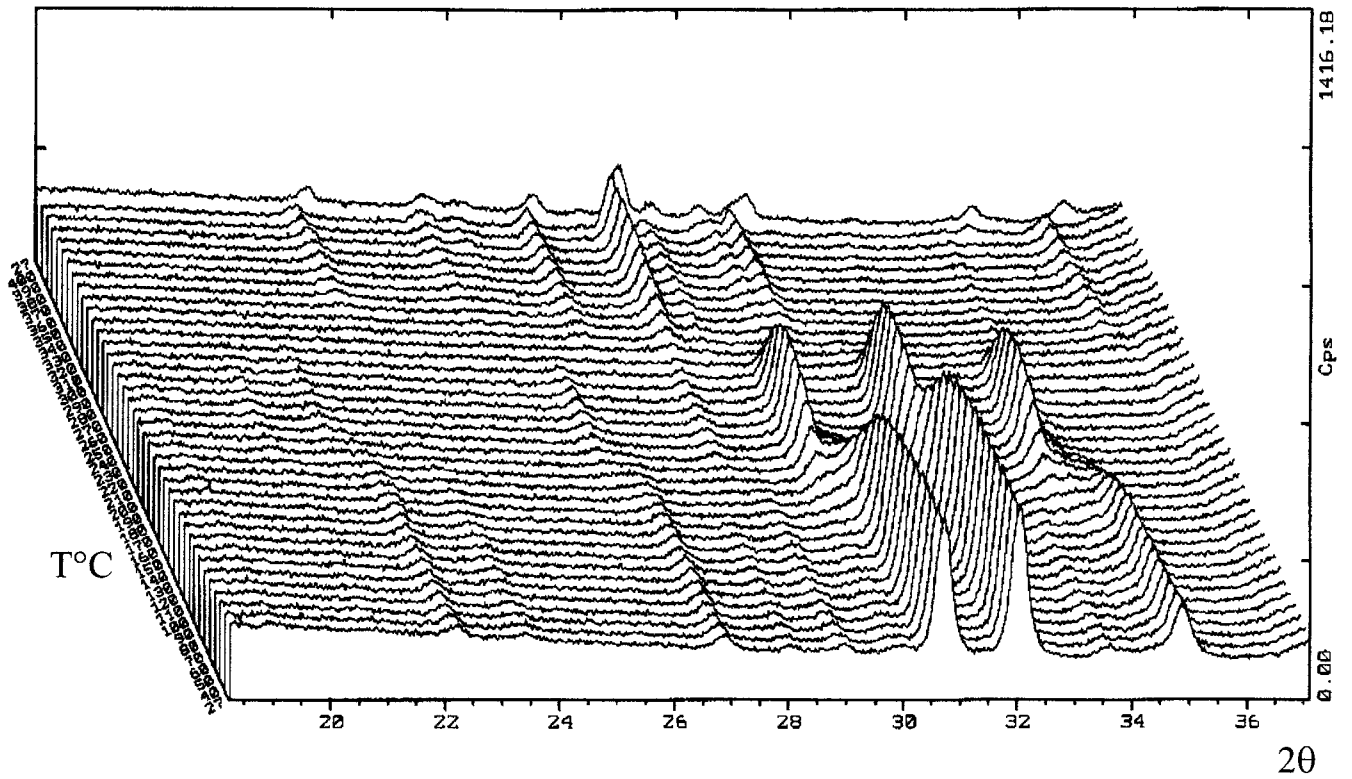

FIG. 12. Powder X-ray diffraction data for $Sr_4Ru_{3.05}O_{12}$ over the temperature range $20 < T < 400°C$, under a ($10\%H_2$, $90\%N_2$) flow.

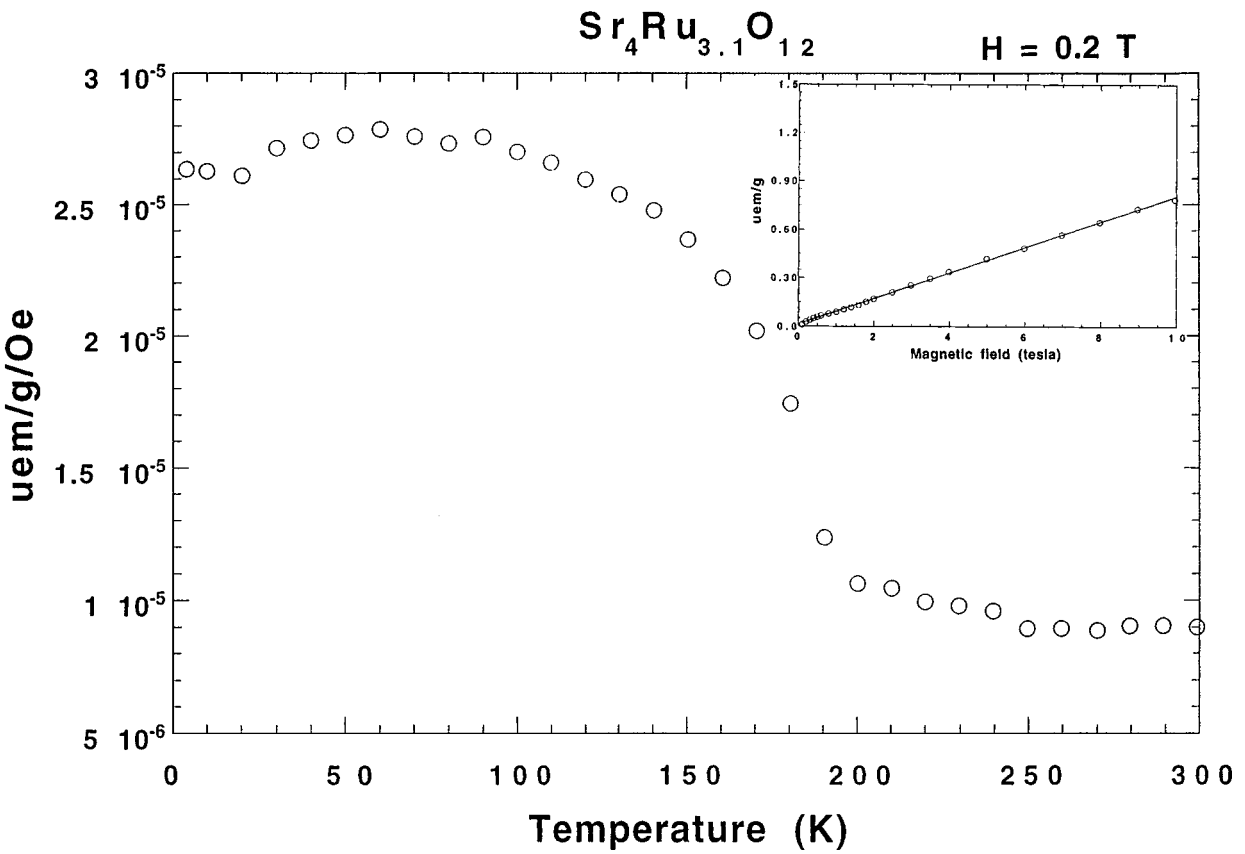

FIG. 13. Thermal variation of the magnetic susceptibility under H = 0.2 T and magnetization variation with H at $T = 10$ K for $Sr_4Ru_{3.05}O_{12}$.

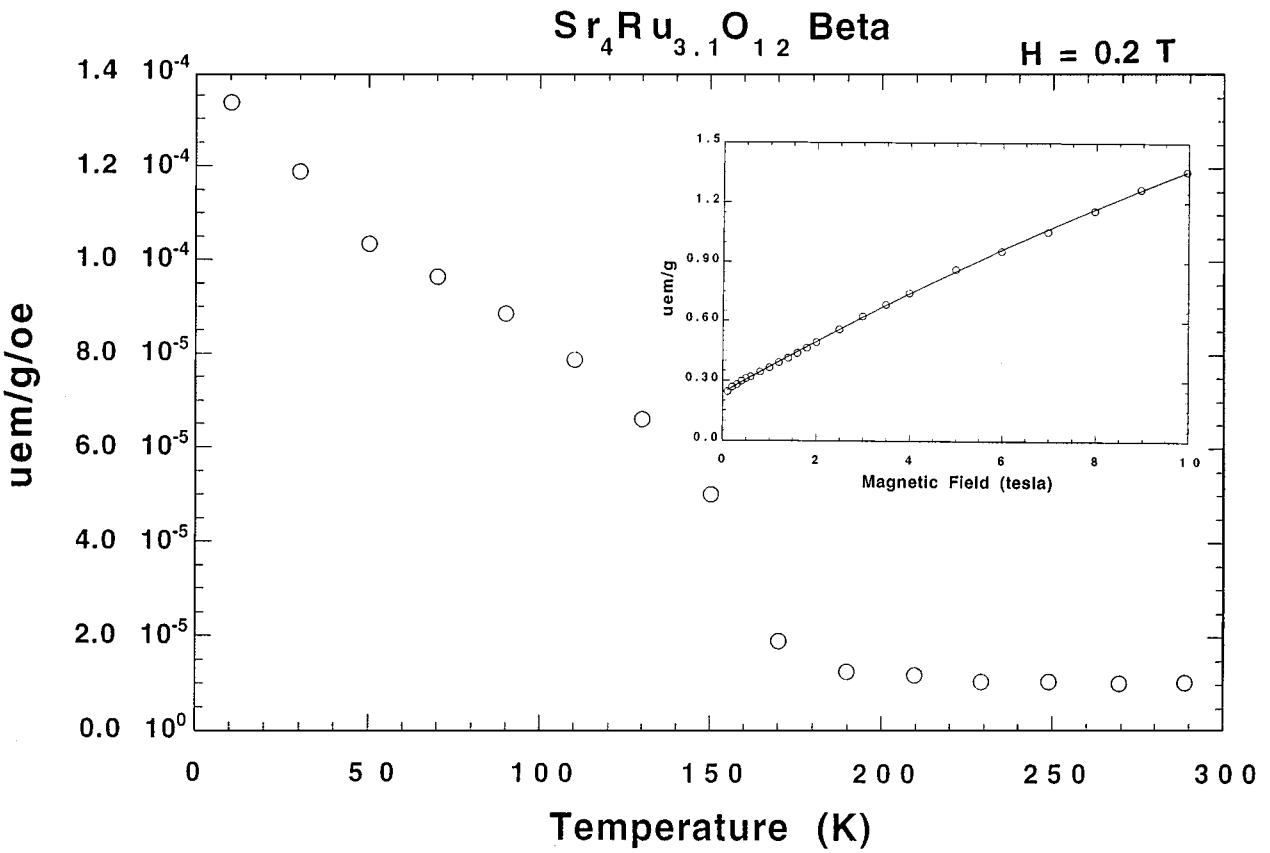

FIG. 14. Thermal variation of the magnetic susceptibility under H = 0.2 T and magnetization variation with H at $T = 10$ K for β-$Sr_4Ru_{3.05}O_{12}$.

ACKNOWLEDGMENTS

We gratefully acknowledge the support of EMAT Laboratory, Antwerpen Belgium, for the high-resolution imaging work. We also express our thanks to Dr. D. Fruchart from the Laboratoire de Cristallographie CNRS Grenoble for his help on the magnetic measurements and for his helpful discussions.

REFERENCES

1. J. Darriet and M. A. Subramanian, *J. Mater. Chem.* **5**(4), 543 (1995).
2. J. J. Randall and R. Ward, *J. Am. Chem. Soc.* **81,** 2629 (1959).
3. C. Dussarrat, J. Fompeyrine, and J. Darriet, *Eur. J. Solid State Inorg. Chem.* **32,** 2 (1995).
4. HK Müller Buschbaum and J. Wilkens, *Z. Anorg. Allg. Chem.* **590,** 161 (1990).
5. T. L. Popova, N. G. Kisel', V. P. Karlov, and V. I. Krivobok, *Russian J. Inorg, Chem.* **26** (11), 1613 (1981).
6. G. Nowogrocki, F. Abraham, J. Tréhoux, and D. Thomas, *Acta Crystallogr. B* **32,** 2413 (1976).
7. J. C. Joubert and J. Chevenas, *J. Solid State Chem.* **27,** 29 (1979).
8. J. De Meulenaer and H. Tompa, *Acta Crystallogr.* **19,** 1014 (1965).
9. P. Lighfoot and P. D. Battle, *J. Solid State Chem.* **89,** 174 (1990).
10. H. U. Schaller and S. Kemmler-Sack, *Z. Anorg. Allg. Chem.* **473,** 178 (1981).
11. J. Darriet, M. Drillon, G. Villeneuve, and P. Hagenmuller, *Z. Anorg. Allg. Chem.* **508,** 93 (1984).
12. H. W. Zandbergen and D. J. W. Ijdo, *Acta Crystallogr. C* **40,** 919 (1984).
13. P. D. Battle, S. H. Kim, and A. V. Ponell, *J. Solid State Chem.* **101,** 161 (1992).
14. C. Dussarrat, J. Fompeyrine, and J. Darriet, *Eur. J. Solid State Inorg. Chem.* **31,** 289 (1994).
15. Seung-Tae Hong and Arthur W. Sleight, *J. Solid State Chem.* **128,** 251 (1997).
16. A. M. Abakumov, G. Van Tendeloo, A. A. Scheglov, R. V. Shpanchenko, and E. V. Antipov, *J. Solid State Chem.* **125,** 102 (1996).
17. R. V. Shpanchenko, L. Nistor, G. Van Tendeloo, J. Van Landuyt, and S. Amelinckx, *J. Solid State Chem.* **114,** 560 (1995).
18. J. Darriet, F. Grasset, and P. D. Battle, *Mater. Res. Bull.* **32,** 139 (1997).